AD683911

Reproduced by the
CLEARINGHOUSE
for Federal Scientific & Technical
Information Springfield Va. 22151

AD683911

FINITE PLATE BENDING ELEMENTS IN POLAR CO-ORDINATES

by

MERVYN D. OLSON, GARRY M. LINDBERG, HELEN A. TULLOCH

A. H. Hall, Head
Structures and Materials Section

F. R. Thurston
Director

SUMMARY

Two finite elements for plate bending in polar co-ordinates are derived. One element is in the form of a circular sector and the other is in the form of an annular sector. The former element has nine degrees of freedom, while the latter has twelve, the degrees of freedom in each case being a displacement and two slopes at each element corner.

The method is checked with several numerical examples. The static deflections of an annular plate and a complete circular plate, both loaded by single concentrated forces, are analyzed and the results compared with exact solutions. Calculations of the free vibrations of complete circular plates are also carried out and compared with exact solutions.

TABLE OF CONTENTS

	Page
SUMMARY	(iii)
TABLES	(iv)
ILLUSTRATIONS	(v)
SYMBOLS	(vi)
1.0 INTRODUCTION	1
2.0 THEORETICAL FORMULATION	2
2.1 Circular Sector Finite Element	2
2.2 Annular Sector Finite Element	6
3.0 NUMERICAL APPLICATIONS	7
3.1 Point Load on Annular Plate	8
3.2 Point Load on Circular Plate	8
3.3 Vibration of Circular Plates	9
4.0 CONCLUDING REMARKS	10
5.0 REFERENCES	10

TABLES

Table		Page
I	Stiffness Matrix $[K_1]/D$ for Circular Sector Finite Element	11
II	Mass Matrix $[M_1]/\rho h\, r_0^2$ for Circular Sector Finite Element	12
III	Transformation Matrix $[T]$ Between Corner Displacements and Polynomial Coefficients for Annular Sector Finite Element	13
IV	Stiffness Matrix $[k]/D$ for Annular Sector Finite Element in Terms of Polynomial Coefficients	14
V	Mass Matrix $[m]/\rho h\beta$ for Annular Sector Finite Element in Terms of Polynomial Coefficients	15
VI	Displacement under Concentrated Load for Clamped-Free Annular Plate	16
VII	Displacements $wD/P \times 10^7$ of Free Edge of Clamped-Free Annular Plate	16

TABLES (Cont'd)

Table		Page
VIII	Displacement under Concentrated Load for Clamped Circular Plate	17
IX	Various Displacements $wD/P \times 10^3$ of Clamped Circular Plate	17
X	Non-Dimensional Frequencies $\sqrt{\rho h/D}\ \omega R^2$ for Clamped Circular Plate, R = 1.0	18
XI	Non-Dimensional Frequencies $\sqrt{\rho h/D}\ \omega R^2$ for Simply Supported Circular Plate, R = 1.0	19
XII	Non-Dimensional Frequencies $\sqrt{\rho h/D}\ \omega R^2$ for Free Circular Plate, R = 1.0	20

ILLUSTRATIONS

Figure		Page
1	Circular Sector Finite Element	21
2	Polynomial Interpolation Functions	22
3	Trigonometric Interpolation Functions	23
4	Annular Sector Finite Element	24
5	Point Loaded Annular Plate Configuration	25
6	Finite Element Assemblages for One-Half Annular Plate	26
7	Displacement Distributions for Clamped-Free Annular Plate Under Point Load	27
8	Point Loaded Circular Plate Configuration	28
9	Finite Element Assemblages for One-Half Circular Plate	29
10	Displacement Distributions for Clamped Circular Plate Under Point Load	30
11	Finite Element Assemblages for Circular Plate Vibrations	31

SYMBOLS

Symbol	Definition
a, b	Plate dimensions, Fig. 5 and 8
a_1 --- a_{12}	Polynomial coefficients, eq. 13
$\{A\}$	Column vector of polynomial coefficients, eq. 15
D	Plate flexural rigidity = $Eh^3/12\,(1-\nu^2)$
E	Young's modulus
h	Plate thickness
H_{01}, H_{02}, H_{11}, H_{12}	Interpolation functions, eq. 4
$[k]$, $[K_1]$	Stiffness matrices, Tables I and IV
$[K_2]$	Stiffness matrix, eq. 20
$[m]$, $[M_1]$	Mass matrices, Tables II and V
$[M_2]$	Mass matrix, eq. 21
P	Concentrated load, Fig. 5 and 8
q	Distributed loading on plate, eq. 1
r	Radial co-ordinate
r_0, r_1, r_2	Element dimensions, Fig. 1 and 4
t	Time
T	Kinetic energy, eq. 2
$[\bar{\ }]$	Transformation matrix, Table III
V	Potential energy, eq. 1
w	Transverse displacement of plate
w_r, w_θ	$\partial w/\partial r$, $\partial w/\partial \theta$, respectively
$\{X_1\}$, $\{X_2\}$	Displacement vectors, eq. 10 and 12
β	Element included angle, Fig. 1 and 4
θ	Azimuthal co-ordinate

SYMBOLS (Cont'd)

Symbol	Definition
ν	Poisson's ratio
ρ	Plate material density
φ_1, φ_2	Trigonometric interpolation functions, eq. 6
ω	Frequency

FINITE PLATE BENDING ELEMENTS IN POLAR CO-ORDINATES

1.0 INTRODUCTION

The finite element method of structural analysis is now firmly established as a powerful technique for handling difficult problems in solid mechanics. Finite elements have been developed in many shapes and for varied applications, the most numerous being the rectangular and triangular plate elements for both bending and plane stress configurations. A good review of the state of the art can be found in the text by Zienkiewicz (Ref. 1), but even this book is becoming outdated by the rapidly advancing field.

The simplest element shapes for plate problems are obviously a triangle and rectangle with three and four nodes, respectively. Rectangular elements are somewhat limited in their boundary shape applicability, whereas triangular elements may be used to represent almost any shape of boundary. However, for problems with curved boundaries, this use of triangular elements means that the curved boundary is being approximated by a series of straight line segments. Further, with some of the more sophisticated elements being developed today, the error introduced by this approximation may well be the limiting factor in some solutions.

Hence, there appears to be a need for elements with curved boundaries. A start in this direction has been made by Ergatoudis et al. in Reference 2, wherein quadrilateral plane stress elements with various curved sides are developed. It would be useful to have this approach extended to bending applications as well. In particular, there is a large class of problems involving circular arc boundaries that are difficult to handle by ordinary analytical means. Problems commonly encountered in jet engines, such as the vibrations of turbine discs and turning vanes, are but two examples.

In the present work, a method for handling such problems is considered. Two plate bending finite elements are developed in polar co-ordinates, which may be joined together in various combinations with rectangular elements to fit a large number of boundary shapes. The first element has three nodal corners and is in the shape of a segment of a circle. The second element has four nodal corners and is in the shape of a segment of an annulus. The transverse displacement and two slopes are used as the degrees of freedom at each element nodal corner. Displacement functions are derived for each element, and the stiffness and mass matrices are obtained by substituting these displacements into the strain and kinetic energy integrals from plate theory.

These elements are fully compatible with the well-known twelve degree of freedom nonconforming rectangular plate elements (Ref. 1). That is, either of the polar co-ordinate elements developed herein may be joined to one of these rectangular elements by equating the displacement and edgewise slope degrees of freedom at the ends of a common boundary. The transverse displacement will then be continuous across such a junction, but the normal slope will, in general, not be continuous there. This is consistent with the fact that these rectangular elements are not conforming. Hence, these polar co-ordinate elements, when combined with the rectangular elements, provide a powerful method for handling a variety of plate bending problems encountered in practical applications.

In the present work, numerical calculations are carried out only with combinations of the polar co-ordinate elements. The examples are chosen primarily as tests of the elements. The static deflection of an annular plate and a complete circular plate, both loaded by single concentrated forces, are analyzed, and the results compared with exact solutions. Finally, calculations of the free vibrations of complete circular plates with clamped, simply supported, and free boundaries are carried out.

2.0 THEORETICAL FORMULATION

The stiffness, mass, and load matrices for the finite element method are most easily obtained from calculations of potential and kinetic energies. Once the displacement functions for a particular finite element have been established, they may be substituted directly into the potential and kinetic energy integrals.

For classical bending of isotropic plates, the potential energy for an element in polar co-ordinates is given by (page 346, Ref. 3)

$$V = \int_0^{\beta} \int_{r_1}^{r_2} \left\{ \frac{D}{2} \left[\left(\frac{\partial^2 w}{\partial r^2} + \frac{1}{r}\frac{\partial w}{\partial r} + \frac{1}{r^2}\frac{\partial^2 w}{\partial \theta^2} \right)^2 - 2(1-\nu)\frac{\partial^2 w}{\partial r^2}\left(\frac{1}{r}\frac{\partial w}{\partial r} + \frac{1}{r^2}\frac{\partial^2 w}{\partial \theta^2} \right) + 2(1-\nu)\left(\frac{1}{r}\frac{\partial^2 w}{\partial r \partial \theta} - \frac{1}{r^2}\frac{\partial w}{\partial \theta} \right)^2 \right] - wq \right\} r\, dr\, d\theta \tag{1}$$

where q is the external loading on the plate element, and D and ν are the customary flexural rigidity and Poisson's ratio, respectively.

The kinetic energy for an element in polar co-ordinates is simply

$$T = \frac{1}{2} \int_0^{\beta} \int_{r_1}^{r_2} \rho h \left(\frac{\partial w}{\partial t} \right)^2 r\, dr\, d\theta \tag{2}$$

where ρ is the material density and h the plate thickness. Making the usual assumption of sinusoidal dependence on time yields

$$T = \frac{\omega^2}{2} \int_0^{\beta} \int_{r_1}^{r_2} \rho h\, w^2\, r\, dr\, d\theta \tag{3}$$

where ω is the frequency of oscillation.

The displacement functions for the two finite elements developed herein are presented in Sections 2.1 and 2.2.

2.1 Circular Sector Finite Element

The first finite element configuration to be considered is shown in Figure 1.

The element is a sector of a circular plate of radius r_0 with an included angle β. The corners are numbered 1 to 3, as shown.

It has become common practice in developing plate bending finite elements to use at least the displacement and two slopes as generalized co-ordinates at each corner of the element. This allows the displacement of the element to vary cubically along any edge. Hence, for the present configuration, this suggests the use of at least the following nine generalized co-ordinates: w_{r12}, w_{r13}, w_1, $w_{\theta 2}$, $w_{\theta 2}$, w_2, w_{r3}, $w_{\theta 3}$ and w_3, where $w_r = \partial w/\partial r$, and $w_\theta = \partial w/\partial \theta$. The single number subscripts denote the corners of the element shown in Figure 1, and w_{r1j} is the slope $\partial w/\partial r$ at corner 1 in the direction of corner j, for j = 2 or 3.

Now a displacement function for this element must be selected. One simple approach to developing a suitable displacement function for this finite element configuration appears to be through the use of interpolation formulas. The merit of this approach for developing rectangular finite elements has been clearly demonstrated in Reference 4. The interpolation formulas used herein are some of the Hermite polynomials, and are

$$
\begin{aligned}
H_{01}(x; a) &= \frac{1}{a^3}(2x^3 - 3ax^2 + a^3) \\
H_{02}(x; a) &= \frac{1}{a^3}(3ax^2 - 2x^3) \\
H_{11}(x; a) &= \frac{1}{a^2}(x^3 - 2ax^2 + a^2 x) \\
H_{12}(x; a) &= \frac{1}{a^2}(x^3 - ax^2)
\end{aligned}
\tag{4}
$$

Note that the bracketed superscript 1 that usually accompanies each $H_{ij}(x)$ has been omitted for simplicity. Plots of these functions are shown in Figure 2. It may be observed that the H_{01} and H_{02} functions have unit value at x = 0 and x = a, respectively; zero value at x = a and x = 0, respectively; and zero slope at both x = 0 and x = a. On the other hand, the H_{11} and H_{12} functions are zero at both x = 0 and x = a, but have unit slope at x = 0 and x = a, respectively. Appropriate combinations of these functions are then used with each generalized co-ordinate; for instance, for a rectangular plate (Ref. 4) the functions that accompany a typical corner displacement are

$$w_1 \; H_{01}(x; a) \; H_{01}(y; b)$$

and with a typical slope are

$$w_{x1} \; H_{11}(x; a) \; H_{01}(y; b)$$

For this circular sector element the displacement may be assumed in

the form

$$w(r, \theta) = w_{r12} H_{11}(r; r_0) H_{01}(\theta; \beta) + w_{r13} H_{11}(r; r_0) H_{02}(\theta; \beta) + w_1 H_{01}(r; r_0) + \ldots\ldots \quad (5)$$

It may be seen that this form provides the proper dependence on the generalized coordinates; for example, the first term provides an acceptable dependence on w_{r12} in that $H_{11}(0; r_0) = 0$, $d H_{11}/dr(0; r_0) = 1$ and $H_{01}(0; \beta) = 1$. However, upon closer inspection, it is seen that the first two terms of expression (5) contain linear terms in r, which represent an infinite bending moment at $r = 0$. This therefore precludes the use of expression (5).

Since there is no way to avoid linear terms in r and still retain the slope degrees of freedom at $r = 0$, different interpolation functions must be found for the θ dependence. It is logical to use the trigonometric functions $\sin\theta$ and $\cos\theta$ in these interpolation functions, since $r \sin\theta$ and $r \cos\theta$ are harmonic functions. Hence, the following trigonometric functions are found to be satisfactory

$$\begin{aligned} \varphi_1(\theta) &= \cos\theta - \cot\beta \sin\theta \\ \varphi_2(\theta) &= \sin\theta/\sin\beta \end{aligned} \quad (6)$$

Typical plots of these two functions are shown in Figure 3 for a few values of the included angle β. It may be seen that φ_1 has unit value at $\theta = 0$ and is zero at $\theta = \beta$, while φ_2 is zero at $\theta = 0$ and has unit value at $\theta = \beta$. Unfortunately, the slopes are, in general, non-zero at either $\theta = 0$ or $\theta = \beta$. These functions have the additional disadvantage that their distributions between $\theta = 0$ and β are not independent of β. However, it is very difficult to find any better functions that are still compatible with the linear term in r. Consequently, the functions φ_1 and φ_2 are used in the present derivation by assuming that w_{r12} and w_{r13} contribute to the element displacement in the following way

$$w(r, \theta) = \left[w_{r12} \varphi_1(\theta) + w_{r13} \varphi_2(\theta)\right] H_{11}(r; r_0) + w_1 H_{01}(r; r_0) + \ldots\ldots \quad (7)$$

It may be noted that the form of equation (7) does represent well-behaved bending moments at $r = 0$.

One further aspect of the displacement expression (7) should be noted here. Differentiating expression (7) with respect to θ and setting $\theta = 0$, yields the circumferential slope along the element edge 1 - 2. It may be seen that this slope depends on w_{r13}, since, in general, $\partial\varphi_2/\partial\theta$ is non-zero at $\theta = 0$. This means that the normal slope along the element edge 1 - 2 is not independent of the displacements along the element edge 1 - 3. Similarly, it may be seen that the normal slope along the edge 1 - 3 is not independent of the edge 1 - 2. This implies that the element will not be of the conforming type, since the normal slopes will not be continuous along the radii between adjacent elements. However, it must be emphasized that this does not preclude

the displacements being continuous between adjacent elements.

Finally, since the element cannot be conforming, it is sufficient to use the nine generalized co-ordinates suggested earlier and to assume the element displacement in the form

$$
\begin{aligned}
w(r, \theta) = w_1 H_{01}(r; r_0) &+ \left[w_{r12}\, \varphi_1(\theta) + w_{r13}\, \varphi_2(\theta)\right] H_{11}(r; r_0) \\
&+ \left[w_{r2}\, H_{01}(\theta; \beta) + w_{r3}\, H_{02}(\theta; \beta)\right] H_{12}(r; r_0) \\
&+ \left[w_{\theta 2}\, H_{11}(\theta, \beta) + w_{\theta 3}\, H_{12}(\theta; \beta)\right] H_{02}(r; r_0) \\
&+ \left[w_2\, H_{01}(\theta; \beta) + w_3\, H_{02}(\theta; \beta)\right] H_{02}(r; r_0) \qquad (8)
\end{aligned}
$$

Note that w is a cubic function of r throughout the element. Furthermore, along the edge 1 - 2 ($\theta = 0$), this cubic variation is uniquely defined by w_{r12}, w_1, w_{r2}, and w_2. The analogous result also holds for the edge 1 - 3. Hence, the displacement will be continuous along the common boundary between adjacent elements, provided their displacements and slopes at $r = 0$ and r_0 are set equal on that boundary. It may also be seen from equation (8) that along the circular edge 2 - 3 ($r = r_0$), w is a cubic function of θ and depends only on $w_{\theta 2}$, w_2, $w_{\theta 3}$, and w_3.

To find the stiffness matrix for e element, the displacement function given by equation (8) is now substituted into the strain energy part of equation (1), and the integration over the element is carried out. Note that for this circular sector finite element, the integration over r is from $r_1 = 0$ to $r_2 = r_0$. This integration yields the strain energy in the form

$$U = \frac{1}{2} \left\{X_1\right\}^T \left[K_1\right] \left\{X_1\right\} \qquad (9)$$

where $\left\{X_1\right\}$ is the column vector

$$\left\{X_1\right\}^T = \left(w_{r12}, w_{r13}, w_1, w_{r2}, w_{\theta 2}, w_2, w_{r3}, w_{\theta 3}, w_3\right) \qquad (10)$$

and $\left[K_1\right]$ is the 9 × 9 stiffness matrix given in Table I. The mass matrix is found in a similar manner by substituting equation (8) into equation (3). This yields the kinetic energy in the form

$$T = \frac{\omega^2}{2} \left\{X_1\right\}^T \left[M_1\right] \left\{X_1\right\} \qquad (11)$$

where $\left[M_1\right]$ is the 9 × 9 mass matrix given in Table II. The consistent load matrix for the element may be obtained by evaluating the wq portion in the integral of equation (1).

2.2 Annular Sector Finite Element

The next finite element configuration to be considered is shown in Figure 4. The element is a sector of an annular plate with inside radius r_1, outside radius r_2, and an included angle β. The corners are numbered 1 to 4 as shown.

A primary objective in the derivation of this element is to make it consistent and compatible with the circular sector element of the previous Section. This will allow the two kinds of elements to be put together for the solution of problems involving portions of circular plates that include the centre of curvature. Therefore, it will be sufficient to use the displacement and two slopes at each corner as the generalized co-ordinates for the element. This will allow the displacement to be cubic in r along edges 1 - 2 and 3 - 4, and cubic in θ along the curved edges 1 - 4 and 2 - 3. Hence, the displacement will be continuous between elements with a common boundary, provided the corner displacements are made equal at the ends of that boundary, but the slope normal to that boundary will, in general, not be continuous across it. The displacement vector for the annular sector finite element then becomes the twelve-term column vector

$$\left\{X_2\right\}^T = \left(w_{r1}, w_{\theta 1}, w_1, w_{r2}, \ldots, w_{r3}, \ldots, w_{r4}, \ldots\right) \tag{12}$$

where the subscripts 1 to 4 denote the corners of the element as shown in Figure 4.

The displacement function for this element is assumed in the form

$$w(r, \theta) = a_1 + a_2 r + a_3\theta + a_4 r\theta + a_5 r^2 + a_6\theta^2 + a_7 r^2\theta + a_8 r\theta^2 + a_9 r^3 + a_{10}\theta^3 + a_{11} r^3\theta + a_{12} r\theta^3 \tag{13}$$

It may be observed that this function is similar in form to that used for the well-known twelve degree of freedom rectangular plate bending element (Ref. 1). In this case, the r and θ co-ordinates just replace the x and y cartesian co-ordinates, respectively, used for the rectangular element.

The twelve corner displacements used in equation (12) may now be evaluated from equation (13). Carrying this out leads to the matrix relation

$$\left\{X_2\right\} = \left[T\right] \left\{A\right\} \tag{14}$$

where $\left\{A\right\}$ is the column vector of polynomial coefficients

$$\left\{A\right\}^T = \left(a_1, a_2, a_3, \ldots\ldots, a_{12}\right) \tag{15}$$

and $\left[T\right]$ is the 12×12 transformation matrix given in Table III. In principle, this transformation matrix may be inverted, and the polynomial coefficients a_i may be determined as functions of the corner displacements of equation (12). The a_i may then be substituted into equation (13), yielding the displacement function in terms of the

corner displacements. However, carrying out this process and substituting the resulting displacement function into the energy integrals involves an amount of work that is impractical.

An alternative approach, which requires much less effort, is to substitute equation (13) directly into the energy integrals. Carrying out the integrations over the element yields the strain energy in the form

$$U = \frac{1}{2} \left\{A\right\}^T \left[k\right] \left\{A\right\} \tag{16}$$

and the kinetic energy in the form

$$T = \frac{\omega^2}{2} \left\{A\right\}^T \left[m\right] \left\{A\right\} \tag{17}$$

where $\left[k\right]$ and $\left[m\right]$ are the 12 × 12 stiffness and mass matrices given in Tables IV and V, respectively, and $\left\{A\right\}$ is given in equation (15). Eliminating $\left\{A\right\}$ from equations (16) and (17) by means of equation (14) yields

$$U = \frac{1}{2} \left\{X_2\right\}^T \left[K_2\right] \left\{X_2\right\} \tag{18}$$

and

$$T = \frac{\omega^2}{2} \left\{X_2\right\}^T \left[M_2\right] \left\{X_2\right\} \tag{19}$$

where

$$\left[K_2\right] = \left[T^{-1}\right]^T \left[k\right] \left[T^{-1}\right] \tag{20}$$

and

$$\left[M_2\right] = \left[T^{-1}\right]^T \left[m\right] \left[T^{-1}\right] \tag{21}$$

are the required 12 × 12 stiffness and mass matrices, respectively, for the element in terms of the corner displacements. The calculations involved in equations (20) and (21) are carried out on the computer to any desired accuracy. The consistent load matrix for the element is found from the wq integral (see eq. (1)), first in terms of the polynomial coefficient vector $\left\{A\right\}$ and then transformed for the corner displacement vector $\left\{X_2\right\}$ by premultiplying by $\left[T^{-1}\right]^T$.

3.0 NUMERICAL APPLICATIONS

The two finite elements developed in the previous Section are now used to solve several numerical examples. These examples serve to indicate how well the elements work in various types of applications. The problems considered are the

static, nonsymmetric deflections of an annular plate and a complete circular plate, both loaded by point loads and the free vibrations of complete circular plates with simply supported, clamped and free boundaries.

3.1 Point Load on Annular Plate

The first problem considered is that of the static, nonsymmetric deflection of the annular plate shown in Figure 5. The plate is clamped along the inner edge (r = b) and loaded by a concentrated force at the outer boundary (r = a). This annular plate configuration is chosen because it may be modelled with only the annular sector finite elements, and hence provides a check of those elements alone. The concentrated load is known to provide one of the severest tests of the finite element method. The problem is also a convenient one to use here because it has an exact series solution. This series solution, which is given on pages 290 - 292 of Reference 3, was programed, and the exact displacement was calculated for comparison with the finite element solutions.

The finite element calculations were carried out for the particular case discussed in Reference 3: $a = 1.5$, $b = 1.0$, and $\nu = 0.3$. Symmetry about the diameter containing the load was used, so that only one-half of the plate had to be modelled. The four successive refinements of finite element assemblages shown in Figure 6 were used in the calculations. The finite element results for the displacement under the load are given in Table VI, along with the number of degrees of freedom used in each calculation. The exact solution is also presented in the Table. The radial and circumferential displacement distributions obtained from the 4×24 grid of finite elements are plotted in Figure 7 along with the exact ones.

Table VI shows that the displacement under the load does not converge monotonically with refinement in finite element size. This is not surprising because the finite elements are not of the conforming type. However, the displacements shown in Table VI are still quite accurate and appear to be converging towards the exact value as the element size becomes quite small. It should be noted that even though the displacement under the load predicted by the 1×6 grid of elements was quite close to the exact value, the circumferential displacement distribution away from the load was very inaccurate. This is shown in Table VII, where numerical results are given for the displacement of the free edge at various circumferential locations. These results serve to illustrate the type of convergence obtained away from the point load. At $\theta = 180°$, this convergence appears to be quite slow, but it may be noted that the displacement there is six orders of magnitude smaller than under the load ($\theta = 0$). In summary, it appears that the annular sector finite elements work very well for the type of problem considered here.

3.2 Point Load on Circular Plate

The next problem considered is that of the static, nonsymmetric deflection of the complete circular plate shown in Figure 8. The plate is clamped around the outer boundary (r = a) and is loaded by a single concentrated force P at r = b. The exact solution for this problem is given by equation (197) on Page 293 of Reference 3.

The modelling of this plate requires the use of both the annular and circular sector finite elements developed herein. Symmetry about the diameter containing the load is again used, so that only one-half of the plate is solved. The numerical calculations are carried out for $a = 1.0$, $b = 0.5$, and $\nu = 0.3$, using the three finite

element assemblages shown in Figure 9.

The numerical results for the displacement under the load are presented in Table VIII, along with the numbers of degrees of freedom used in each calculation. The displacements predicted for a few other positions on the plate are given in Table IX. Radial and circumferential displacement distributions obtained from the 6 × 8 grid calculations are shown in Figure 10. All these results exhibit a high accuracy, but unfortunately the convergence is somewhat disappointing. For example, the 2 × 4 and 4 × 6 grid predictions for the displacement under the load are only in error by about one percent, and appear to be converging in that the 4 × 6 grid answer is more accurate than the 2 × 4 one. However, the 6 × 8 grid prediction is in error by about two percent, and the sign of this error is different from that of the former ones. Since the results in the previous Section, using the annular sector finite elements by themselves, appeared to be well-behaved, it is suspected that the erratic convergence behaviour observed here is probably caused by the circular sector finite elements. As pointed out in Section 2.1, the trigonometric interpolation functions used in developing these elements changed shape as the included angle β was changed. However, in the limit of very small included angle, these functions approach a constant straight line shape. Hence, it is expected that this erratic convergence behaviour would disappear if the finite element assemblages were increasingly refined. In summary then, even though the convergence is somewhat erratic, the numerical accuracy is still quite satisfactory for most applications.

3.3 Vibration of Circular Plates

The free vibrations of complete circular plates with clamped, simply supported, and free outer edges are now analyzed with the present finite elements. These final applications serve to check out the consistent mass matrices for the elements. The calculations are carried out for a plate radius of unity and Poisson's ratio equal to 0.33, using the three finite element assemblages shown in Figure 11. As indicated in the Figure, the 3 × 12 grid solution was separated into two sub-problems by using symmetry about a diameter. This was done in order to keep the eigenvalue problems to a manageable size.

The non-dimensional frequency predictions for the first few vibration modes are presented in Tables X, XI, and XII for the three problems. The exact solutions are taken from Reference 5. It may be seen that, in some cases, two different eigenvalues were obtained for apparently the same vibration mode. Upon close inspection of the predicted mode shapes it was found that the predicted frequencies depended on whether or not the radial nodal lines fell between or along the finite element junctions. For example, in the 2 × 8 grid predictions of Modes Seven, for the clamped and simply supported plates, and Mode Five for the free plate, the nodal lines were along the element junctions for the low eigenvalues and mid-way between them for the high ones. The same trend was found to hold for the other non-repeated eigenvalues. This peculiar effect may again be associated with the circular sector finite elements and their special interpolation functions. It may be noted that the differences between the non-repeating eigenvalues appear to decrease as the modelling is refined, until the final predictions are quite close to the exact values. Again, very little can be said about the particular convergence of these calculations because the elements are not of the conforming type.

4.0 CONCLUDING REMARKS

A finite element method for plate bending elements in polar co-ordinates has been presented. Two elements were developed - one in the form of a circular plate sector and the other in the form of an annular plate sector. The application of these elements to several static and dynamic numerical examples indicated the accuracy to be expected with the method.

These elements may be combined with rectangular elements for the analysis of a variety of plate bending problems heretofore considered unsolvable.

5.0 REFERENCES

1. Zienkiewicz, O. C. — The Finite Element Method in Structural and Continuum Mechanics. McGraw-Hill, London, 1967.

2. Ergatoudis, I., Irons, B. M., Zienkiewicz, O. C. — Curved, Isoparametric, 'Quadrilateral' Elements for Finite Element Analysis. Int. Journal of Solids and Structures, Vol. 4, Jan. 1968, p. 31-42.

3. Timoshenko, S. P., Woinowsky-Krieger, S. — Theory of Plates and Shells. 2nd ed. McGraw-Hill, New York, 1959.

4. Bogner, F. K., Fox, R. L., Schmit, L. A., Jr. — The Generation of Inter-Element-Compatible Stiffness and Mass Matrices by the Use of Interpolation Formulas. IN Przemieniecki, J. S., Bader, R. M., et al., eds. Matrix Methods in Structural Mechanics. AFFDL-TR-66-80, Wright-Patterson AFB, Ohio, Nov. 1966, p. 397-443.

5. McLeod, A. J., Bishop, R. E. D. — The Forced Vibration of Circular Flat Plates. Mechanical Engineering Science Monograph No. 1, Inst. of Mech. Engineers, London, March 1965.

TABLE I

STIFFNESS MATRIX $\left[K_1\right]/D$ FOR CIRCULAR SECTOR FINITE ELEMENT

k_1								
k_2	k_1							
k_3	k_3	k_4						
k_5	k_6	k_7	k_8					
k_9	k_{10}	k_{11}	k_{12}	k_{13}				
k_{14}	k_{15}	k_{16}	k_{17}	k_{18}	k_{19}			
k_6	k_5	k_7	k_{20}	k_{21}	k_{22}	k_8		
$-k_{10}$	$-k_9$	$-k_{11}$	$-k_{21}$	k_{23}	k_{24}	$-k_{12}$	$-k_{13}$	
k_{15}	k_{14}	k_{16}	k_{22}	$-k_{24}$	k_{25}	k_{17}	$-k_{18}$	k_{19}

SYMMETRICAL

where

$$k_1 = \beta \csc^2\beta - \frac{1+2\nu}{3}\cot\beta; \quad k_2 = \left[\frac{1+2\nu}{3} - \beta\cot\beta\right]\csc\beta; \quad k_3 = \frac{3+\nu}{r_0}\left[\csc\beta - \cot\beta\right]; \quad k_4 = \frac{9\beta}{r_0^2};$$

$$k_5 = -\frac{1}{\beta^3}\left[\left(6 + \frac{7+\nu}{6}\beta^2\right)\beta\cot\beta + 6\beta\csc\beta - 12\right]; \quad k_6 = \frac{1}{\beta^3}\left[\left(6 + \frac{7+\nu}{6}\beta^2\right)\beta\csc\beta + 6\beta\cot\beta - 12\right];$$

$$k_7 = \frac{9\beta}{4r_0}; \quad k_8 = \frac{13(13+4\nu)}{140}\beta + \frac{1}{\beta^3} + \frac{1}{5\beta}; \quad k_9 = \frac{1}{r_0\beta^2}\left[\frac{11+\nu}{3}\beta^2 + 6\beta\left(\csc\beta + 2\cot\beta\right) - 18\right];$$

$$k_{10} = \frac{6}{r_0\beta^2}\left[\beta\left(\cot\beta + 2\csc\beta\right) - 3\right]; \quad k_{11} = \frac{1}{r_0^2}\left[2 - \nu - \frac{3}{4}\beta^2\right]; \quad k_{12} = \frac{1}{r_0}\left[\frac{6-43\nu}{30} - \frac{2}{\beta^2} - \frac{33}{140}\beta^2\right];$$

$$k_{13} = \frac{2}{r_0^2}\left[\frac{3}{70}\beta^3 + \frac{3}{\beta} - \frac{3-\nu}{15}\beta\right]; \quad k_{14} = \frac{1}{r_0\beta^3}\left\{\left[18 + (3+\nu)\beta^2\right]\beta\cot\beta + 18\beta\csc\beta - 36\right\};$$

$$k_{15} = -\frac{1}{r_0\beta^3}\left\{\left[18 + (3+\nu)\beta^2\right]\beta\csc\beta + 18\cot\beta - 36\right\}; \quad k_{16} = -\frac{9\beta}{2r_0^2}; \quad k_{17} = \frac{1}{r_0}\left[\frac{2(1-3\nu)}{5\beta} - \frac{4}{\beta^3} - \frac{117}{70}\beta\right];$$

$$k_{18} = \frac{1}{r_0^2}\left[\frac{33}{70}\beta^2 + \frac{9}{\beta^2} - \frac{23-11\nu}{10}\right]; \quad k_{19} = \frac{2}{r_0^2}\left[\frac{117}{70}\beta + \frac{9}{\beta^3} - \frac{3(3-\nu)}{5\beta}\right]; \quad k_{20} = \frac{117+36\nu}{280}\beta - \frac{1}{\beta^3} - \frac{1}{5\beta};$$

$$k_{21} = \frac{1}{r_0}\left[\frac{39}{280}\beta^2 - \frac{2}{\beta^2} + \frac{1-3\nu}{10}\right]; \quad k_{22} = \frac{1}{r_0^2}\left[\frac{4}{\beta^3} - \frac{81}{140}\beta - \frac{2(1-3\nu)}{5\beta}\right]; \quad k_{23} = \frac{1}{r_0^2}\left[\frac{3}{\beta} - \frac{9}{140}\beta^3 + \frac{3-\nu}{30}\beta\right];$$

$$k_{24} = \frac{1}{r_0^2}\left[\frac{9}{\beta^2} - \frac{39}{140}\beta^2 - \frac{3-\nu}{10}\right]. \quad k_{25} = \frac{3}{r_0^2}\left[\frac{27}{70}\beta - \frac{6}{\beta^3} + \frac{2(3-\nu)}{5\beta}\right]$$

TABLE II

MASS MATRIX $\left[M_1\right]/\rho h\, r_0^{\,2}$ FOR CIRCULAR SECTOR FINITE ELEMENT

k_1								
k_2	k_1							
k_3	k_3	k_4						
k_5	k_6	k_7	k_8					
k_9	k_{10}	k_{11}	k_{12}	k_{13}				
k_{14}	k_{15}	k_{16}	k_{17}	k_{18}	k_{19}			
k_6	k_5	k_7	k_{20}	k_{21}	k_{22}	k_8		
$-k_{10}$	$-k_9$	$-k_{11}$	$-k_{21}$	k_{23}	k_{24}	$-k_{12}$	k_{13}	
k_{15}	k_{14}	k_{16}	k_{22}	$-k_{24}$	k_{25}	k_{17}	$-k_{18}$	k_{19}

SYMMETRICAL

where

$$k_1 = \frac{r_0^{\,2}}{560}\left(\beta \csc^2\beta - \cot\beta\right); \quad k_2 = \frac{r_0^{\,2}}{560}\csc\beta\left(1 - \beta\cot\beta\right); \quad k_3 = \frac{r_0}{60}\left(\csc\beta - \cot\beta\right); \quad k_4 = \frac{3}{35}\beta;$$

$$k_5 = \frac{r_0^{\,2}}{280}\left[6\beta\csc\beta + \beta\left(6+\beta^2\right)\cot\beta - 12\right]; \quad k_6 = -\frac{r_0^{\,2}}{280}\left[6\beta\cot\beta + \left(6+\beta^2\right)\beta\csc\beta - 12\right];$$

$$k_7 = -\frac{r_0\beta}{140}; \quad k_8 = \frac{13\, r_0^{\,2}\beta}{5880}; \quad k_9 = -\frac{r_0}{60\beta^2}\left[2\beta\left(\csc\beta + 2\cot\beta\right) - 6 + \beta^2\right];$$

$$k_{10} = \frac{r_0}{30\beta^2}\left[\beta\left(\cot\beta + 2\csc\beta\right) - 3\right]; \quad k_{11} = \frac{3\beta^2}{560}; \quad k_{12} = -\frac{11\, r_0\beta^2}{5880}; \quad k_{13} = \frac{2\beta^3}{735};$$

$$k_{14} = -\frac{r_0}{60\beta^3}\left[6\beta\csc\beta + \left(6+\beta^2\right)\beta\cot\beta - 12\right]; \quad k_{15} = +\frac{r_0}{60\beta^3}\left[6\beta\cot\beta + \left(6+\beta^2\right)\beta\csc\beta - 12\right];$$

$$k_{16} = \frac{9\beta}{280}; \quad k_{17} = -\frac{13\, r_0\beta}{980}; \quad k_{18} = \frac{11\beta^2}{735}; \quad k_{19} = \frac{26\beta}{245}; \quad k_{20} = \frac{3\, r_0^{\,2}\beta}{3920}; \quad k_{21} = -\frac{13\, r_0\beta^2}{11760};$$

$$k_{22} = -\frac{9\, r_0\beta}{1960}; \quad k_{23} = -\frac{\beta^3}{490}; \quad k_{24} = -\frac{13\beta^2}{1470}; \quad k_{25} = \frac{9\beta}{245};$$

TABLE III

TRANSFORMATION MATRIX [T] BETWEEN CORNER DISPLACEMENTS AND POLYNOMIAL COEFFICIENTS FOR ANNULAR SECTOR FINITE ELEMENT

0	1	0	0	$2r_1$	0	0	0	$3r_1^2$	0	0	0
0	0	1	r_1	0	0	r_1^2	0	0	0	r_1^3	0
1	r_1	0	0	r_1^2	0	0	0	r_1^3	0	0	0
0	1	0	0	$2r_2$	0	0	0	$3r_2^2$	0	0	0
0	0	1	r_2	0	0	r_2^2	0	0	0	r_2^3	0
1	r_2	0	0	r_2^2	0	0	0	r_2^3	0	0	0
0	1	0	β	$2r_2$	0	$2\beta r_2$	β^2	$3r_2^2$	0	$3\beta r_2^2$	β^3
0	0	1	r_2	0	2β	r_2^2	$2\beta r_2$	0	$3\beta^2$	r_2^3	$3\beta^2 r_2$
1	r_2	β	βr_2	r_2^2	β^2	βr_2^2	$\beta^2 r_2$	r_2^3	β^3	βr_2^3	$\beta^3 r_2$
0	1	0	β	$2r_1$	0	$2\beta r_1$	β^2	$3r_1^2$	0	$3\beta r_1 2$	β^3
0	0	1	r_1	0	2β	r_1^2	$2\beta r_1$	0	$3\beta^2$	r_1^3	$3\beta^2 r_1$
1	r_1	β	βr_1	r_1^2	β^2	βr_1^2	$\beta^2 r_1$	r_1^3	β^3	βr_1^3	$\beta^3 r_1$

TABLE IV

STIFFNESS MATRIX $[k]/D$ FOR ANNULAR SECTOR
FINITE ELEMENT IN TERMS OF POLYNOMIAL COEFFICIENTS

0											
0	k_1										
0	0	k_2									
0	k_3	0	k_4								
0	k_5	0	k_6	k_7							
0	k_8	k_9	k_{10}	k_{11}	k_{12}						
0	k_{13}	k_{14}	k_{15}	k_{16}	k_{17}	k_{18}					
0	k_{19}	0	k_{20}	k_{21}	k_{22}	k_{23}	k_{24}				
0	k_{25}	0	k_{26}	k_{27}	k_{28}	k_{29}	k_{30}	k_{31}			
0	k_{32}	k_{33}	k_{34}	k_{35}	k_{36}	k_{37}	k_{38}	k_{39}	k_{40}		
0	k_{41}	k_{42}	k_{43}	k_{44}	k_{45}	k_{46}	k_{47}	k_{48}	k_{49}	k_{50}	
0	k_{51}	0	k_{52}	k_{53}	k_{54}	k_{55}	k_{56}	k_{57}	k_{58}	k_{59}	k_{60}

SYMMETRICAL

where

$k_1 = \beta \ln\left(\frac{r_2}{r_1}\right)$; $k_2 = (1-\nu)\beta\left(\frac{1}{r_1^2} - \frac{1}{r_2^2}\right)$; $k_3 = \frac{1}{2}\beta^2 \ln\left(\frac{r_2}{r_1}\right)$; $k_4 = \frac{1}{3}\beta^3 \ln\left(\frac{r_2}{r_1}\right)$; $k_5 = 2(1+\nu)\beta(r_2 - r_1)$; $k_6 = (1+\nu)\beta^2(r_2 - r_1)$;

$k_7 = 4(1+\nu)\beta\left(r_2^2 - r_1^2\right)$; $k_8 = 2\beta\left(\frac{1}{r_1} - \frac{1}{r_2}\right)$; $k_9 = (1-\nu)\beta^2\left(\frac{1}{r_1^2} - \frac{1}{r_2^2}\right)$; $k_{10} = \beta^2\left(\frac{1}{r_1} - \frac{1}{r_2}\right)$; $k_{11} = 4(1+\nu)\beta \ln\left(\frac{r_2}{r_1}\right)$;

$k_{12} = 2\beta\left(\frac{1}{r_2^2} - \frac{1}{r_2^2}\right)\left[1 + \frac{2}{3}(1-\nu)\beta^2\right]$; $k_{13} = (1+\nu)\beta^2(r_2 - r_1)$; $k_{14} = -2(1-\nu)\beta \ln\left(\frac{r_2}{r_1}\right)$; $k_{15} = \frac{2}{3}(1+\nu)\beta^3(r_2 - r_1)$; $k_{16} = 2(1+\nu)\beta^2\left(r_2^2 - r_1^2\right)$;

$k_{17} = 4\nu\beta^2 \ln\left(\frac{r_2}{r_1}\right)$; $k_{18} = 2\beta\left(r_2^2 - r_1^2\right)\left[\frac{1}{2}(1-\nu) + \frac{2}{3}(1+\nu)\beta^2\right]$; $k_{19} = \frac{1}{2}\beta\left(4 + \frac{2}{3}\beta^2\right)\ln\left(\frac{r_2}{r_1}\right)$; $k_{20} = \frac{1}{2}\beta^2\left(2 + \frac{1}{2}\beta^2\right)\ln\left(\frac{r_2}{r_1}\right)$;

$k_{21} = 2(1+\nu)\beta\left(2 + \frac{1}{3}\beta^2\right)(r_2 - r_1)$; $k_{22} = \beta\left(4 + \frac{2}{3}\beta^2\right)\left(\frac{1}{r_1} - \frac{1}{r_2}\right)$; $k_{23} = \frac{1}{2}(1+\nu)\beta^2(4 + \beta^2)(r_2 - r_1)$; $k_{24} = \beta\left(4 + \frac{4}{3}\beta^2 + \frac{1}{5}\beta^4\right)\ln\left(\frac{r_2}{r_1}\right)$;

$k_{25} = 3\beta\left(\frac{1}{2} + \nu\right)\left(r_2^2 - r_1^2\right)$; $k_{26} = \frac{3}{2}\left(\frac{1}{2} + \nu\right)\beta^2\left(r_2^2 - r_1^2\right)$; $k_{27} = 6(1+\nu)\beta\left(r_2^3 - r_1^3\right)$; $k_{28} = 6(1+2\nu)\beta(r_2 - r_1)$; $k_{29} = 3(1+\nu)\beta^2\left(r_2^3 - r_1^3\right)$;

$k_{30} = \left(\frac{1}{2} + \nu\right)\beta\left(6 + \beta^2\right)\left(r_2^2 - r_1^2\right)$; $k_{31} = \frac{9}{4}(5+4\nu)\beta\left(r_2^4 - r_1^4\right)$; $k_{32} = 3\beta^2\left(\frac{1}{r_1} - \frac{1}{r_2}\right)$; $k_{33} = (1-\nu)\beta^3\left(\frac{1}{r_1^2} - \frac{1}{r_2^2}\right)$; $k_{34} = 2\beta^3\left(\frac{1}{r_1} - \frac{1}{r_2}\right)$;

$k_{35} = 6(1+\nu)\beta^2 \ln\left(\frac{r_2}{r_1}\right)$; $k_{36} = 3\beta^2\left(\frac{1}{r_1^2} - \frac{1}{r_2^2}\right)\left[1 + \frac{1}{2}(1-\nu)\beta^2\right]$; $k_{37} = 2(1+3\nu)\beta^3 \ln\left(\frac{r_2}{r_1}\right)$; $k_{38} = \frac{3}{2}\beta^2\left(4 + \beta^2\right)\left(\frac{1}{r_1} - \frac{1}{r_2}\right)$; $k_{39} = 9(1+2\nu)\beta^2(r_2 - r_1)$;

$k_{40} = 2\beta^3\left[3 + \frac{9}{10}(1-\nu)\beta^2\right]\left(\frac{1}{r_1^2} - \frac{1}{r_2^2}\right)$; $k_{41} = \frac{3}{2}\left(\frac{1}{2} + \nu\right)\beta^2\left(r_2^2 - r_1^2\right)$; $k_{42} = -4(1-\nu)\beta(r_2 - r_1)$; $k_{43} = \left(\frac{1}{2} + \nu\right)\beta^3\left(r_2^2 - r_1^2\right)$;

$k_{44} = 3(1+\nu)\beta^2\left(r_2^3 - r_1^3\right)$; $k_{45} = (10\nu - 1)\beta^2(r_2 - r_1)$; $k_{46} = \beta\left(r_2^3 - r_1^3\right)\left[\frac{4}{3}(1-\nu) + 2(1+\nu)\beta^2\right]$; $k_{47} = \frac{3}{8}(1+2\nu)\beta^2\left(4 + \beta^2\right)\left(r_2^2 - r_1^2\right)$;

$k_{48} = \frac{9}{8}(5+4\nu)\beta^2\left(r_2^4 - r_1^4\right)$; $k_{49} = 2(1+8\nu)\beta^3(r_2 - r_1)$; $k_{50} = 2\left[\frac{3}{8}(5+4\nu)\beta^2 + (1-\nu)\right]\beta\left(r_2^4 - r_1^4\right)$; $k_{51} = \frac{1}{2}\beta^2\left(6 + \frac{1}{2}\beta^2\right)\ln\left(\frac{r_2}{r_1}\right)$;

$k_{52} = \beta^3\left(2 + \frac{1}{5}\beta^2\right)\ln\left(\frac{r_2}{r_1}\right)$; $k_{53} = \frac{1}{2}(1+\nu)\beta^2\left(12 + \beta^2\right)(r_2 - r_1)$; $k_{54} = \frac{1}{2}\beta^2\left(12 + \beta^2\right)\left(\frac{1}{r_1} - \frac{1}{r_2}\right)$; $k_{55} = 2(1+\nu)\beta^3\left(2 + \frac{1}{5}\beta^2\right)(r_2 - r_1)$;

$k_{56} = \frac{1}{2}\beta^2\left(12 + 4\beta^2 + \frac{1}{3}\beta^4\right)\ln\left(\frac{r_2}{r_1}\right)$; $k_{57} = \beta^2\left[\frac{3}{2}(1+2\nu) + \frac{3}{8}(1+2\nu)\beta^2\right]\left(r_2^2 - r_1^2\right)$; $k_{58} = 6\beta^3\left(2 + \frac{1}{5}\beta^2\right)\left(\frac{1}{r_1} - \frac{1}{r_2}\right)$;

$k_{59} = \frac{3}{2}(1+2\nu)\beta^3\left(2 + \frac{1}{5}\beta^2\right)\left(r_2^2 - r_1^2\right)$; $k_{60} = \beta^3\left(12 + \frac{12}{5}\beta^2 + \frac{1}{5}\beta^4\right)\ln\left(\frac{r_2}{r_1}\right)$

TABLE V

MASS MATRIX $[m]/\rho h\beta$ FOR ANNULAR SECTOR FINITE ELEMENT

IN TERMS OF POLYNOMIAL COEFFICIENTS

$\gamma_2/2$											
$\gamma_3/3$	$\gamma_4/4$										
$\beta\gamma_2/4$	$\beta\gamma_3/6$	$\beta^2\gamma_2/6$									
$\beta\gamma_3/6$	$\beta\gamma_4/8$	$\beta^2\gamma_3/9$	$\beta^2\gamma_4/12$								
$\gamma_4/4$	$\gamma_5/5$	$\beta\gamma_4/8$	$\beta\gamma_5/10$	$\gamma_6/6$		SYMMETRICAL					
$\beta^2\gamma_2/6$	$\beta^2\gamma_3/9$	$\beta^3\gamma_2/8$	$\beta^3\gamma_3/12$	$\beta^2\gamma_4/12$	$\beta^4\gamma_2/10$						
$\beta\gamma_4/8$	$\beta\gamma_5/10$	$\beta^2\gamma_4/12$	$\beta^2\gamma_5/15$	$\beta\gamma_6/12$	$\beta^3\gamma_4/16$	$\beta^2\gamma_6/18$					
$\beta^2\gamma_3/9$	$\beta^2\gamma_4/12$	$\beta^3\gamma_3/12$	$\beta^3\gamma_4/16$	$\beta^2\gamma_5/15$	$\beta^4\gamma_3/15$	$\beta^3\gamma_5/20$	$\beta^4\gamma_4/20$				
$\gamma_5/5$	$\gamma_6/6$	$\beta\gamma_5/10$	$\beta\gamma_6/12$	$\gamma_7/7$	$\beta^2\gamma_5/15$	$\beta\gamma_7/14$	$\beta^2\gamma_6/18$	$\gamma_8/8$			
$\beta^3\gamma_2/8$	$\beta^3\gamma_3/12$	$\beta^4\gamma_2/10$	$\beta^4\gamma_3/15$	$\beta^3\gamma_4/16$	$\beta^5\gamma_2/12$	$\beta^4\gamma_4/20$	$\beta^5\gamma_3/18$	$\beta^3\gamma_5/20$	$\beta^6\gamma_2/14$		
$\beta\gamma_5/10$	$\beta\gamma_6/12$	$\beta^2\gamma_5/15$	$\beta^2\gamma_6/18$	$\beta\gamma_7/14$	$\beta^3\gamma_5/20$	$\beta^2\gamma_7/21$	$\beta^3\gamma_6/24$	$\beta\gamma_8/16$	$\beta^4\gamma_5/25$	$\beta^2\gamma_8/24$	
$\beta^3\gamma_3/12$	$\beta^3\gamma_4/16$	$\beta^4\gamma_3/15$	$\beta^4\gamma_4/20$	$\beta^3\gamma_5/20$	$\beta^5\gamma_3/18$	$\beta^4\gamma_5/25$	$\beta^5\gamma_4/24$	$\beta^3\gamma_6/24$	$\beta^6\gamma_3/21$	$\beta^4\gamma_6/30$	$\beta^6\gamma_4/28$

where $\gamma_i = r_2^i - r_1^i$ for $i = 2, 3, ---- 8$

TABLE VI

DISPLACEMENT UNDER CONCENTRATED LOAD FOR

CLAMPED-FREE ANNULAR PLATE

FINITE ELEMENT GRIDS	NUMBER OF DEGREES OF FREEDOM	DISPLACEMENT UNDER LOAD P, wD/P
1 × 6	19	0.050896
2 × 12	74	0.051372
3 × 18	165	0.051027
4 × 24	292	0.050885
EXACT SOLUTION		0.0507180

TABLE VII

DISPLACEMENTS $wD/P \times 10^7$ OF FREE EDGE OF

CLAMPED-FREE ANNULAR PLATE

FINITE ELEMENT GRIDS	ANGULAR POSITION, θ (degrees)					
	30	60	90	120	150	180
1 × 6	83601.	-29847.	-3546.5	1713.7	132.28	-191.42
2 × 12	80564.	-8773.7	-1226.3	156.43	18.019	-5.4920
3 × 18	82446.	-5141.8	-1071.9	56.900	13.695	-1.2304
4 × 24	83338.	-3930.8	-1013.6	30.939	12.008	-0.36776

TABLE VIII

DISPLACEMENT UNDER CONCENTRATED LOAD FOR

CLAMPED CIRCULAR PLATE

FINITE ELEMENT GRIDS	NUMBER OF DEGREES OF FREEDOM	DISPLACEMENT UNDER LOAD P, wD/P
2 × 4	18	0.0113155
4 × 6	63	0.0112715
6 × 8	133	0.0109738
EXACT SOLUTION		0.0111906

TABLE IX

VARIOUS DISPLACEMENTS $wD/P \times 10^3$ OF

CLAMPED CIRCULAR PLATE

FINITE ELEMENT GRIDS	r = 0	r = 0.5 θ = 90°	r = 0.5 θ = 180°
2 × 4	8.5086	3.6035	2.3598
4 × 6	8.1946	3.6995	2.3434
6 × 8	8.1068	3.7350	2.5624
EXACT SOLUTION	8.0259	3.6927	2.3120

TABLE X

NON-DIMENSIONAL FREQUENCIES $\sqrt{\rho h/D}\,\omega R^2$ FOR CLAMPED CIRCULAR PLATE, R = 1.0

MODES	FINITE ELEMENT GRIDS			EXACT SOLUTIONS
	1 × 4	2 × 8	3 × 12	
1. 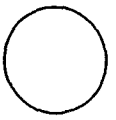	10.247	10.223	10.139	10.24
2. 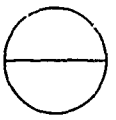	23.664	20.736	20.973	21.25
3. 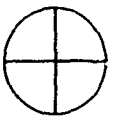		32.919	33.645 23.911	34.8
4. 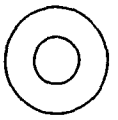		40.249	39.368	39.8
5. 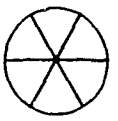		50.917	47.418	51.0
6. 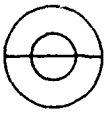		67.583	60.987	60.8
7. 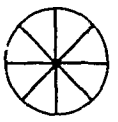		66.234 111.209	62.335 62.341	69.7
8. 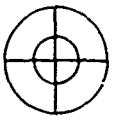		107.07	80.021 81.253	84.6
9. 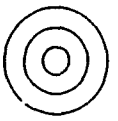		115.15	88.859	89.1

TABLE XI

NON-DIMENSIONAL FREQUENCIES $\sqrt{\rho h/D}\,\omega R^2$ FOR SIMPLY SUPPORTED CIRCULAR PLATE, R = 1.0

MODES	FINITE ELEMENT GRIDS			EXACT SOLUTIONS
	1 × 4	2 × 8	3 × 12	
1. 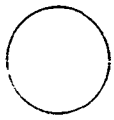	4.9865	4.9795	4.9424	4.97
2. 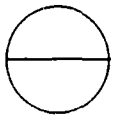	15.373	13.649	13.923	13.91
3. 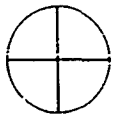	30.673	24.614	25.294 25.459	25.7
4. 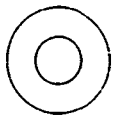	39.655	30.206	29.425	29.7
5. 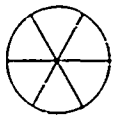		39.553	38.262	39.9
6. 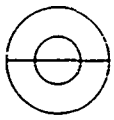		52.920	48.415	48.6
7. 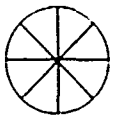		49.475 111.209	53.525 53.528	56.9
8. 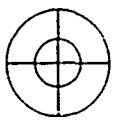		78.801	67.641 68.558	70.1
9. 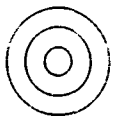		85.780	74.664	74.1

TABLE XII

NON-DIMENSIONAL FREQUENCIES $\sqrt{\rho h/D}\,\omega R^2$ FOR FREE CIRCULAR PLATE, R = 1.0

MODES	FINITE ELEMENT GRIDS			EXACT SOLUTIONS
	1 × 4	2 × 8	3 × 12	
1. 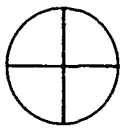	5.3349 9.8543	5.9823	5.9071 5.9405	5.24
2. 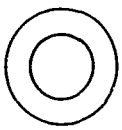	9.0941	9.0818	8.9795	9.06
3. 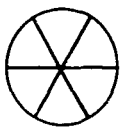	25.155	13.519	12.982	12.25
4. 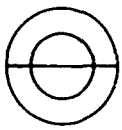	20.916	20.160	20.243	20.5
5. 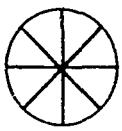		23.597 25.565	23.016	21.5
6. 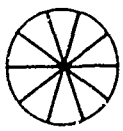		39.919	34.184 34.442	33.1
7. 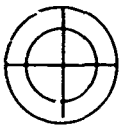		33.269	36.014	35.5
8. 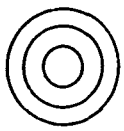		38.721	38.116	38.4

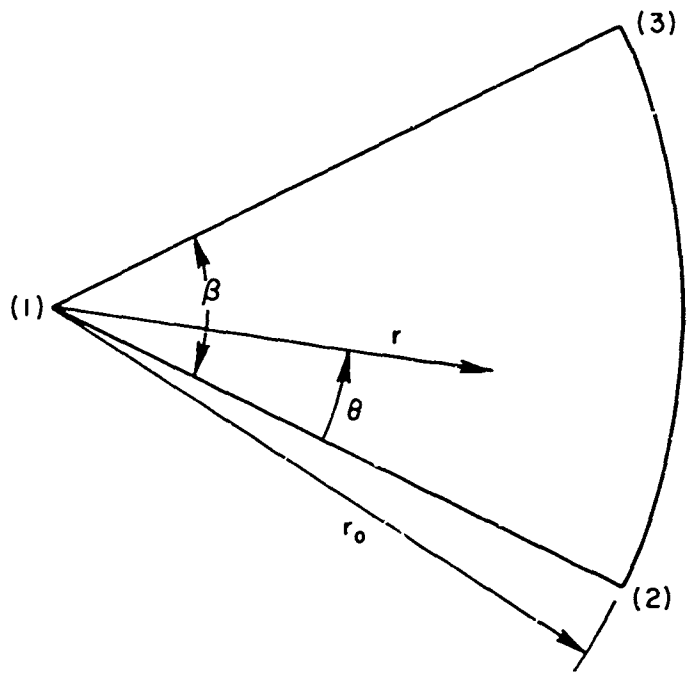

FIG.1: CIRCULAR SECTOR FINITE ELEMENT

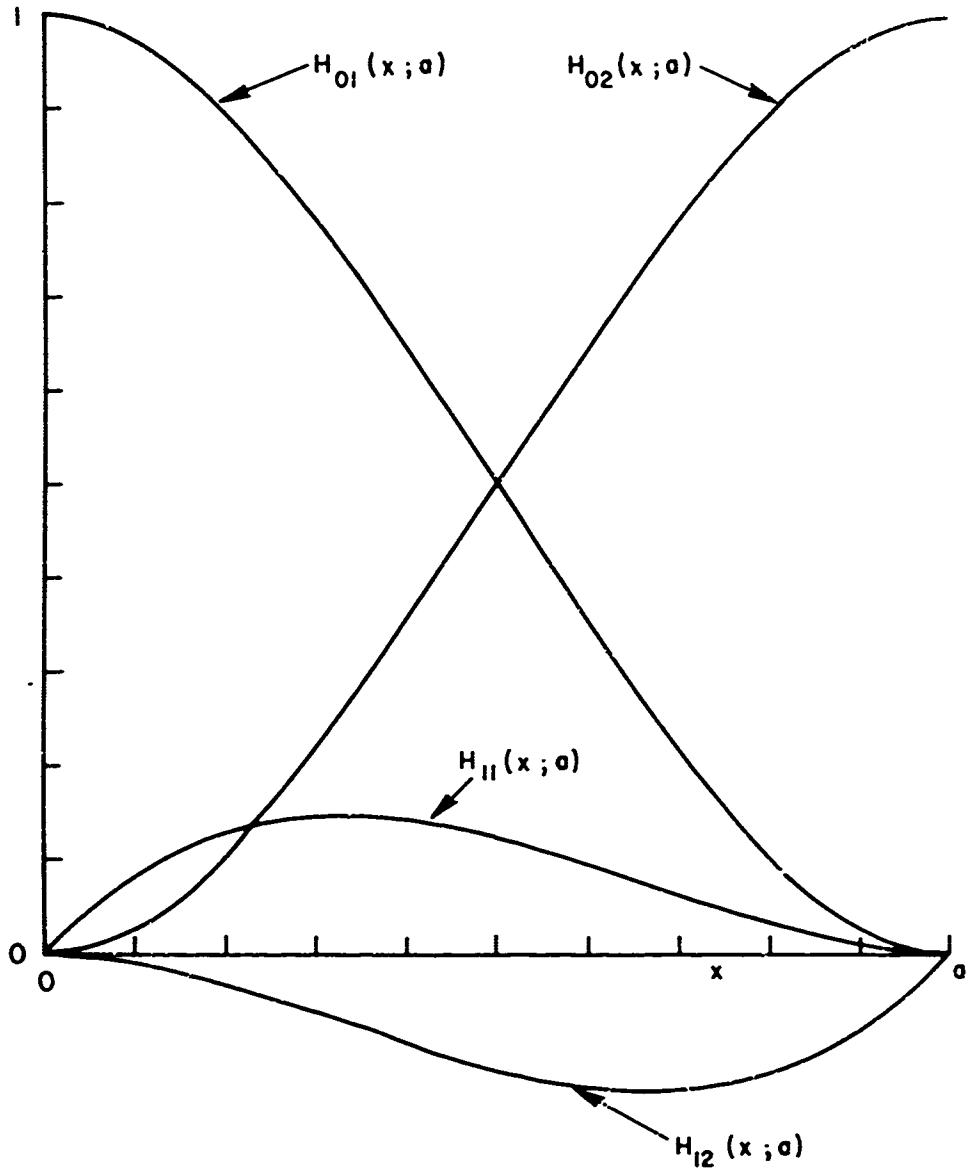

FIG. 2 : POLYNOMIAL INTERPOLATION FUNCTIONS

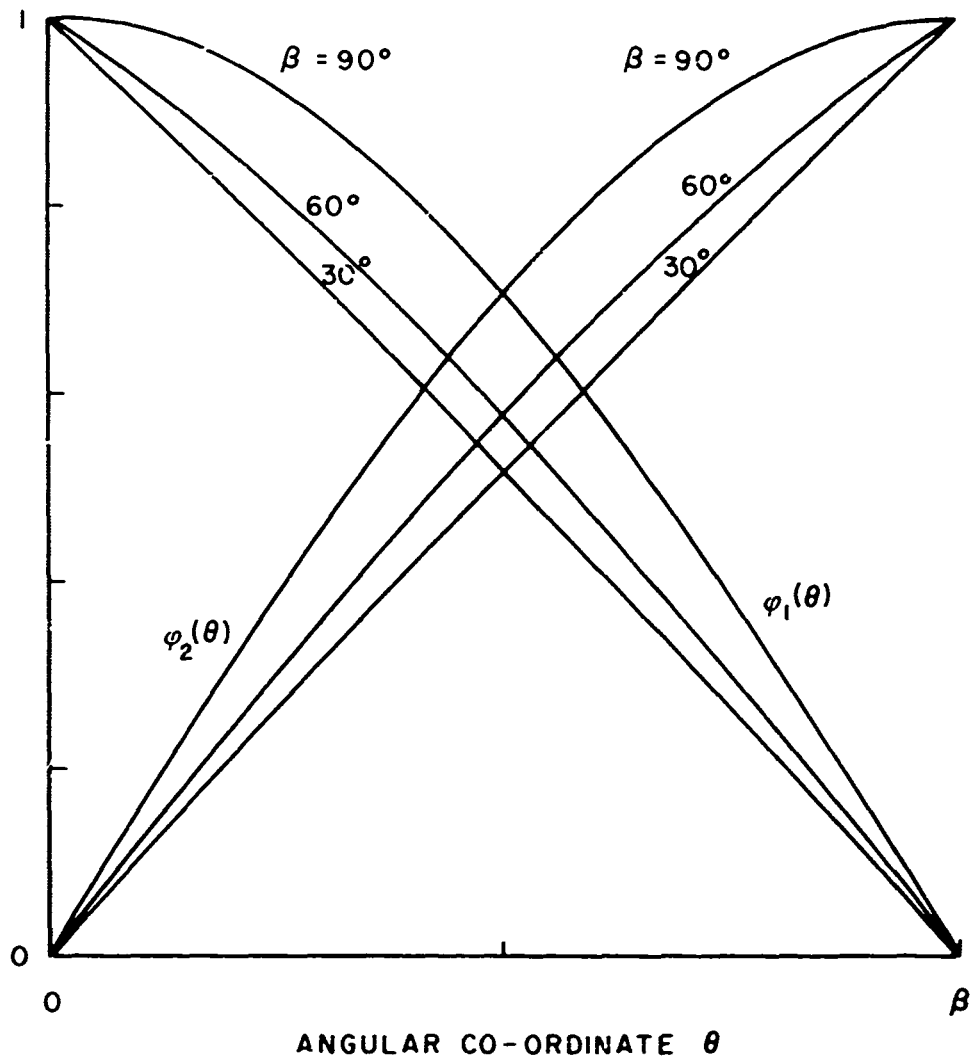

FIG. 3: TRIGONOMETRIC INTERPOLATION FUNCTIONS

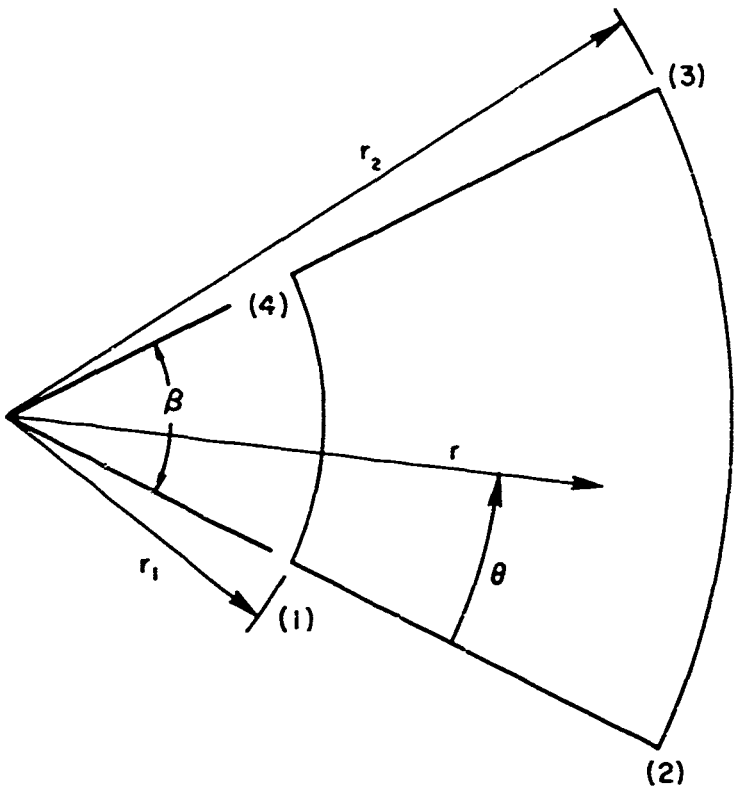

FIG 4: ANNULAR SECTOR FINITE ELEMENT

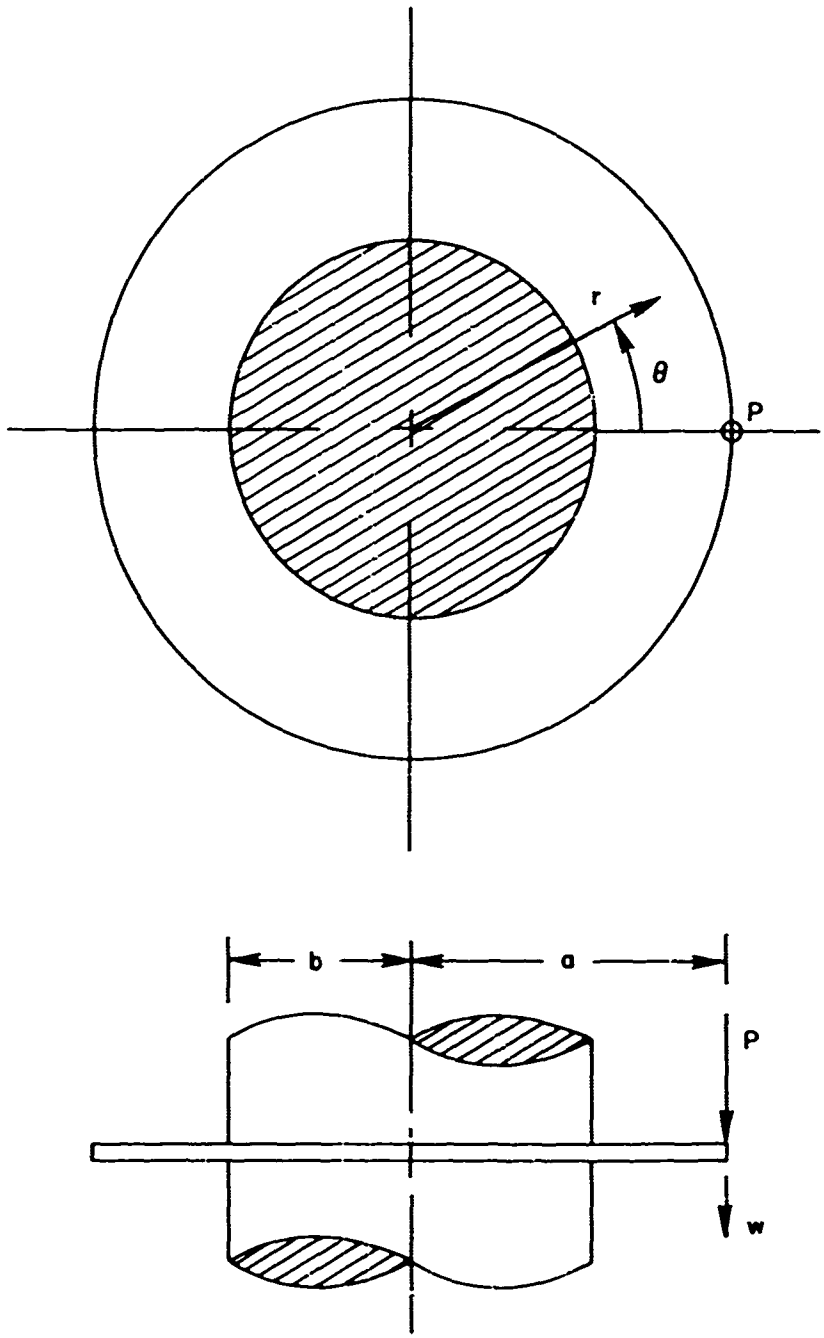

FIG.5: POINT LOADED ANNULAR PLATE CONFIGURATION

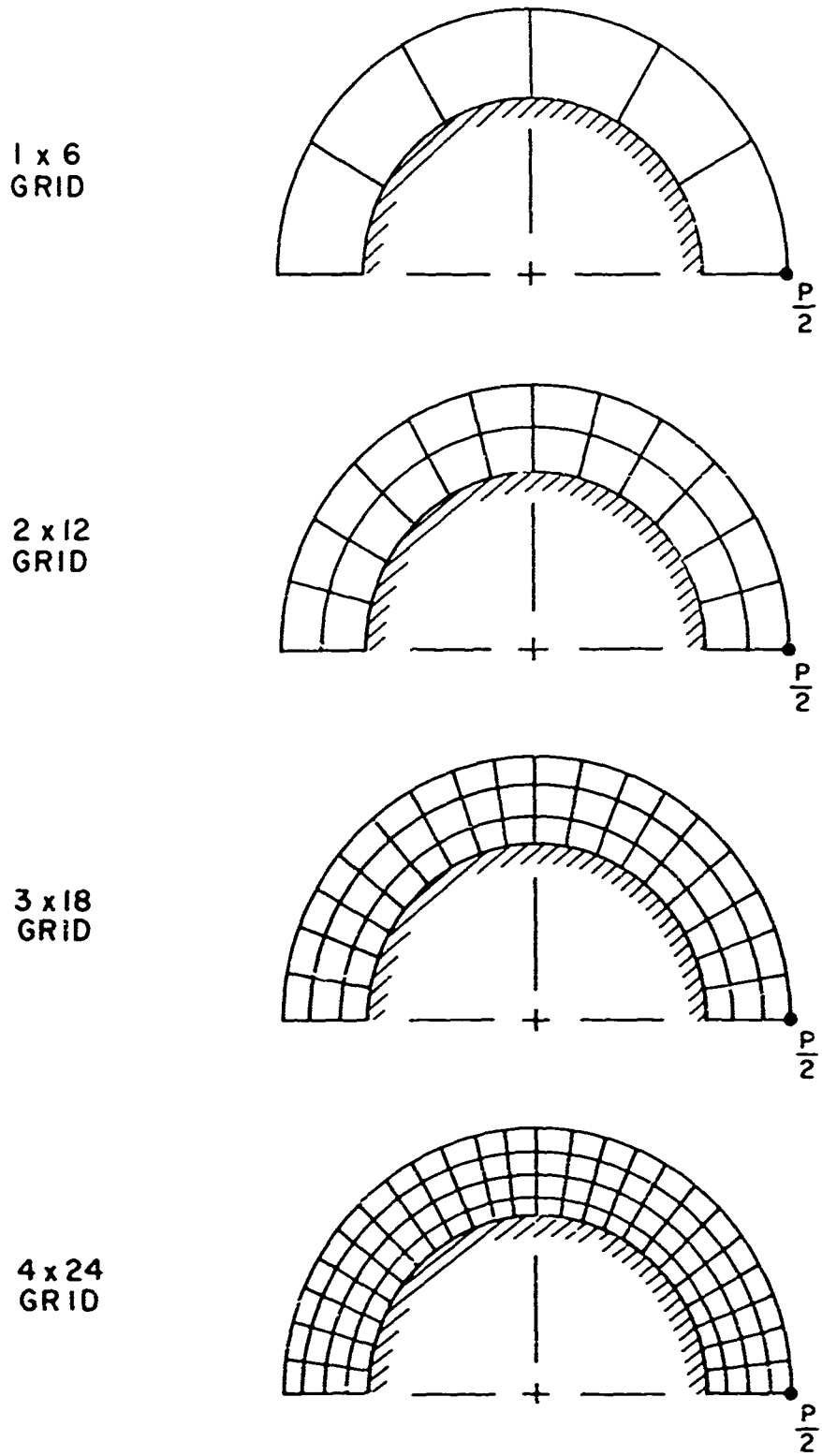

FIG. 6: FINITE ELEMENT ASSEMBLAGES FOR ONE-HALF ANNULAR PLATE

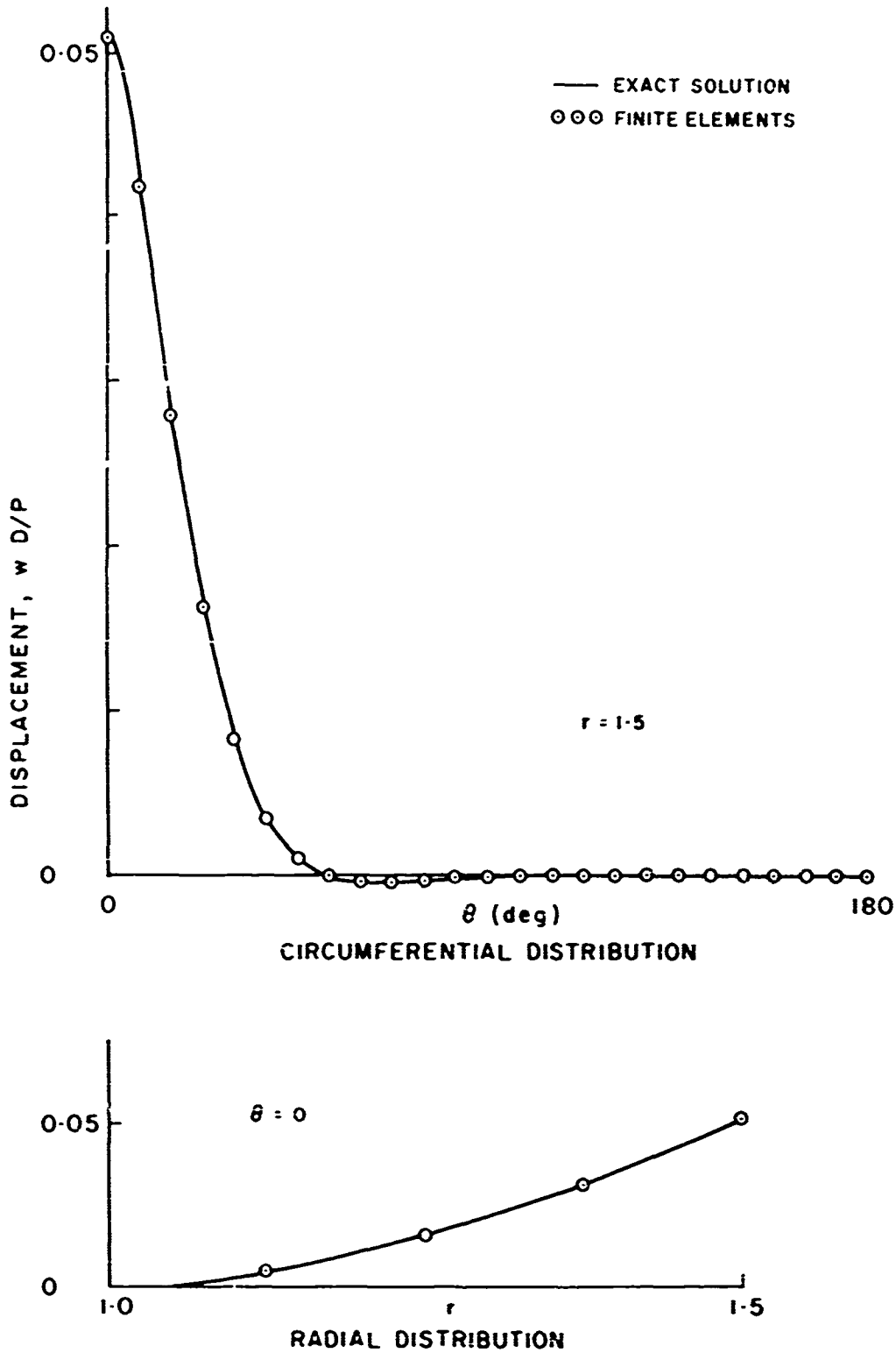

FIG. 7: DISPLACEMENT DISTRIBUTIONS FOR CLAMPED-FREE ANNULAR PLATE UNDER POINT LOAD

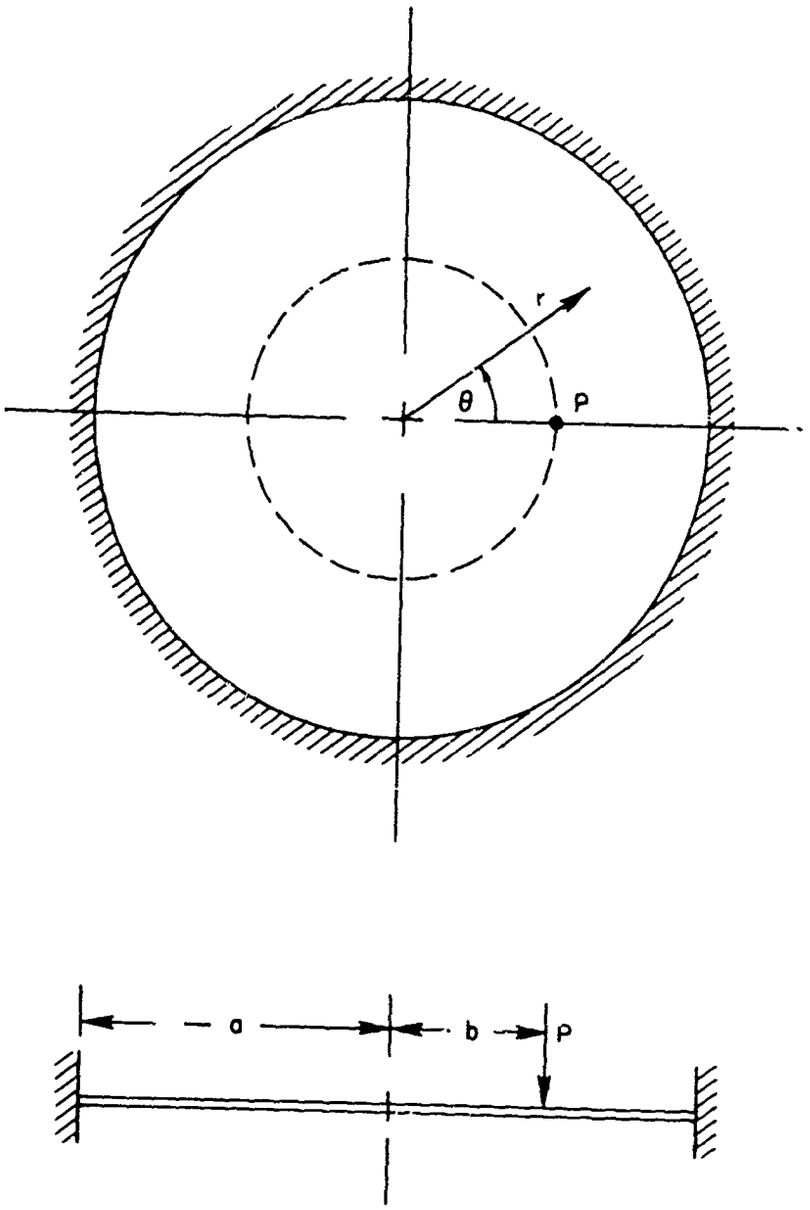

FIG. 8: POINT LOADED CIRCULAR PLATE CONFIGURATION

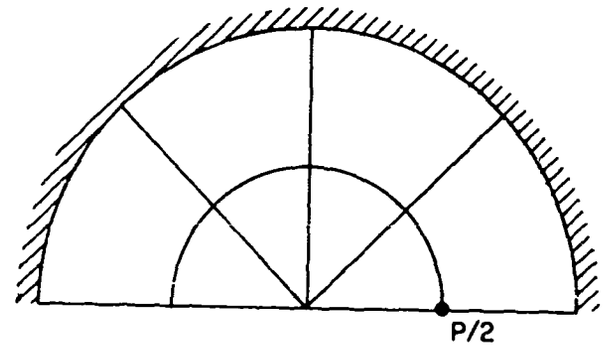

2 x 4 GRID

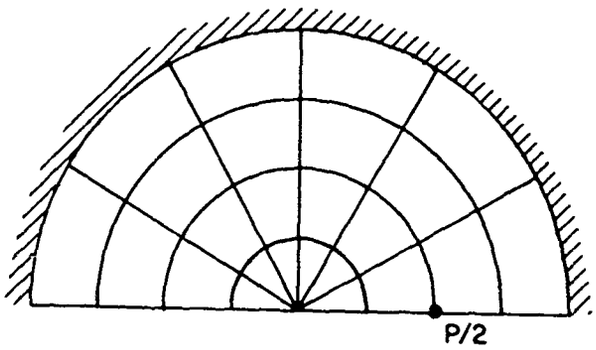

4 x 6 GRID

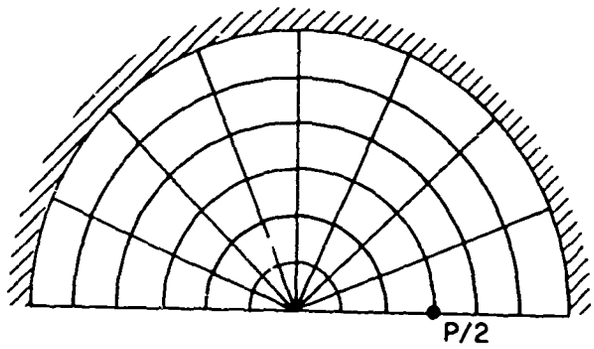

6 x 8 GRID

FIG.9: FINITE ELEMENT ASSEMBLAGES FOR ONE-HALF CIRCULAR PLATE

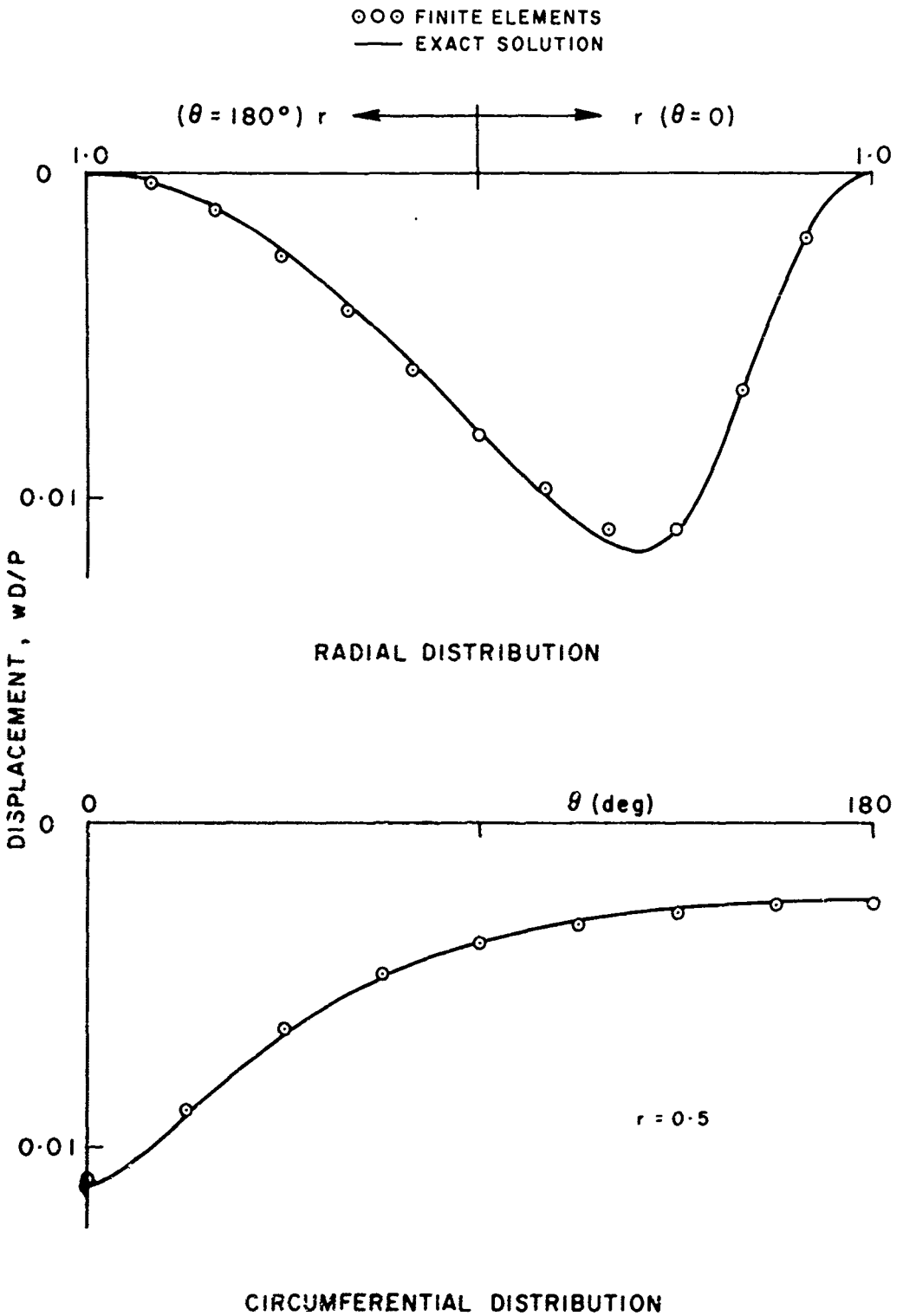

FIG.10: DISPLACEMENT DISTRIBUTIONS FOR CLAMPED CIRCULAR PLATE UNDER POINT LOAD

1 x 4
GRID

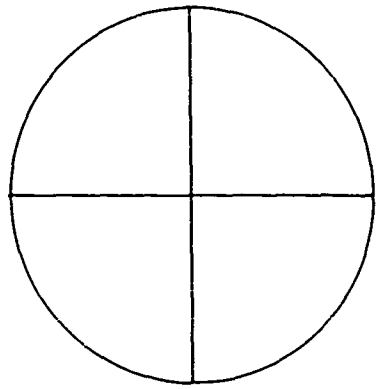

2 x 8
GRID

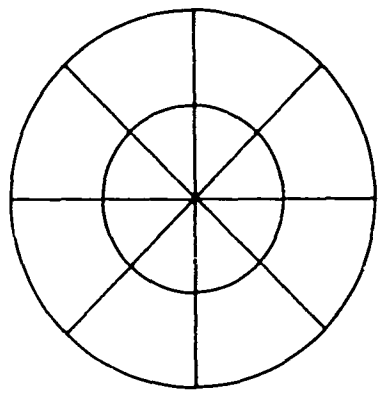

3 x 12
GRID

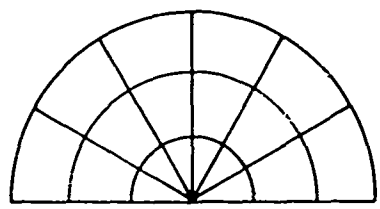

FIG. 11: FINITE ELEMENT ASSEMBLAGES FOR CIRCULAR PLATE VIBRATIONS